

# Centrosome loss or amplification does not dramatically perturb global gene expression in *Drosophila*

Janina Baumbach<sup>1</sup>, Mitchell P. Levesque<sup>2,\*</sup> and Jordan W. Raff<sup>1,‡</sup>

<sup>1</sup>Sir William Dunn School of Pathology, University of Oxford, South Parks Road, Oxford OX1 3RE, UK

<sup>2</sup>Max Planck Institute for Developmental Biology, Spemannstrasse 35, 72076 Tübingen, Germany

\*Present address: University of Zurich Hospital, Gloriastrasse 31, CH-8091 Zurich, Switzerland

‡Author for correspondence (jordan.raff@path.ox.ac.uk)

*Biology Open* 1, 983–993  
doi: 10.1242/bio.20122238  
Received 12th June 2012  
Accepted 29th June 2012

## Summary

Centrosome defects are a common feature of many cancers, and they can predispose fly brain cells to form tumours. In flies, centrosome defects perturb the asymmetric division of the neural stem cells, but it is unclear how this might lead to malignant transformation. One possibility is that centrosome defects might also perturb cellular homeostasis: for example, stress pathways are often activated in response to centrosome defects in cultured cells, and stress contributes to tumorigenesis in some fly models. Here we attempt to assess whether centrosome loss or centrosome amplification perturbs cell physiology *in vivo* by profiling the global transcriptome of *Drosophila* larval brains and imaginal discs that either lack centrosomes or have too many centrosomes. Surprisingly, we find that centrosome loss or

amplification leads to few changes in the transcriptional profile of these cells, indicating that centrosome defects are surprisingly well tolerated by these cells. These observations indicate that centrosome defects can predispose fly brain cells to form tumours without, at least initially, dramatically altering their physiology.

© 2012. Published by The Company of Biologists Ltd. This is an Open Access article distributed under the terms of the Creative Commons Attribution Non-Commercial Share Alike License (<http://creativecommons.org/licenses/by-nc-sa/3.0>).

Key words: Centrosome defects, Centrosome amplification, Tumours

## Introduction

Centrosomes are the major microtubule (MT) organising centres (MTOCs) in many cell types and they are widely believed to have an important role in organising many cell processes such as cell division, the establishment and maintenance of cell polarity and the positioning of organelles within the cell. Centrosomes are also thought to act as “coordination centres” for various cellular pathways, as many cell cycle regulators and checkpoint proteins are concentrated at centrosomes (Hsu and White, 1998; Löffler et al., 2007; Tritarelli et al., 2004). Not surprisingly, centrosome defects have been implicated in a wide range of human diseases, most notably cancer, but more recently also in brain development and in conditions associated with defects in DNA damage repair (Alkuraya et al., 2011; Bakircioglu et al., 2011; Bond and Woods, 2006; Doxsey et al., 2005; Hsu and White, 1998; Lingle et al., 2002; Löffler et al., 2007; Pihan et al., 2003; Takada et al., 2007; Tritarelli et al., 2004).

Given their general importance, the recent demonstration that flies can proceed through the majority of development without centrosomes or with amplified centrosomes in the majority of their cells was very surprising (Basto et al., 2008; Basto et al., 2006). Somatic cell divisions were slowed when centrosomes were missing or amplified (as cells took longer than normal to assemble a bipolar spindle) but almost all cells appeared to ultimately divide normally in a bipolar fashion, although there

was a small, but significant, increase in chromosome segregation errors in these cells. In contrast, asymmetrically dividing larval neuroblasts (NBs) appeared to have considerable difficulty in dividing accurately when centrosomes were either absent or amplified. These large stem-cell-like progenitors normally divide asymmetrically to generate another self-renewing NB, and a smaller ganglion mother cell (GMC) that usually divides only a few more times before terminally differentiating into either a neuron or glial cell (Doe, 2008; Knoblich, 2008). In NBs that either lack centrosomes or have too many centrosomes this division is symmetric ~10–15% of the time (Basto et al., 2008; Basto et al., 2006). These symmetric divisions appear to give rise to two NB-like daughters (Basto et al., 2008; Lee et al., 2006a; Wang et al., 2006).

Intriguingly, brain cells that either lack or have too many centrosomes are predisposed to form tumours in abdominal transplantation assays (Basto et al., 2008; Castellanos et al., 2008). It is widely believed that this tumourigenesis is driven by the failure in asymmetric NB divisions (Castellanos et al., 2008; Gonzalez, 2007), and, in support of this possibility, mutations in genes encoding the asymmetrically distributed neural cell fate determinants Numb, Prospero and Brat also lead to tumourigenesis (Bello et al., 2006; Betschinger et al., 2006; Caussinus and Gonzalez, 2005; Lee et al., 2006a; Lee et al., 2006b; Wang et al., 2006). While a failure in asymmetric division

can clearly lead to an expansion of the NB pool and so to over-proliferation, it is unclear how centrosome malfunction promotes malignant transformation. One possibility is that the relatively mild chromosome segregation defects induced by centrosome loss or amplification could facilitate the accumulation of mutations (Basto et al., 2008; Basto et al., 2006); however, mutations causing large-scale genome instability do not lead to brain tumour induction (Castellanos et al., 2008). In addition, it has been suggested that transcriptional and/or epigenetic changes may be required to promote malignant transformation in these brains (Knoblich, 2010). Interestingly, centrosome defects are known to increase cellular stress *in vitro* (Mikule et al., 2007; Srsen et al., 2006; Uetake et al., 2007), and stress can promote tumorigenesis in at least some *Drosophila* tumour models (Rossi and Gonzalez, 2011; Wu et al., 2010).

Thus, although flies with centrosome defects appear capable of progressing through most of development relatively normally, it remains possible that cell physiology could be significantly perturbed by these defects (Gonzalez, 2008). Here, we have attempted to address how centrosome loss or amplification might perturb cell physiology *in vivo*. We reasoned that any stress induced by these centrosome defects would likely induce physiological changes, at least some of which should be detectable as transcriptional changes. An analysis of global gene expression would, therefore, be a reasonable first readout of any possible changes in cell physiology. Indeed, many other *Drosophila* tumour models such as *l(3)mbt*, *brat*, *aurA*, *lgl* and *aPKC<sup>CAAX</sup>* lead to large-scale changes in gene expression *in situ* (Carney et al., 2012; Janic et al., 2010).

Here we have compared the global transcriptome of brains and imaginal discs from animals that either lack centrosomes (due to mutations in the core centriole duplication proteins *DSas-4* or *DSas-6*) (Basto et al., 2006; Peel et al., 2007; Rodrigues-Martins et al., 2007) or that have amplified centrosomes in the majority of their cells (due to the overexpression of *Sak/Plk4*) (Basto et al., 2008). Surprisingly, we found that these centrosome defects lead to very few changes to the global transcriptome, strongly suggesting that centrosome loss or amplification, *per se*, does not dramatically perturb *Drosophila* cell physiology *in vivo*.

## Results

**Centrosome defects in *DSas-4* and *DSas-6* mutant and *SakOE* larval brains lead to an increase in brain size**

To compare the transcriptome of normal cells to cells that either lack centrosomes or have too many centrosomes we used *DSas-4* or *DSas-6* mutant lines that lack centrosomes in >95% of their cells (Fig. 1A,B) (Basto et al., 2006; Peel et al., 2007; Rodrigues-Martins et al., 2007), or a *Sak/Plk4* overexpressing line (hereafter *SakOE*) that has extra centrosomes in ~70% of its cells (Basto et al., 2008) (Fig. 1A,C). In addition, we also compared the size of the brain lobes in these lines. As expected, brain size was slightly, but significantly, enlarged when compared to wild type in all three lines (Fig. 1D – note that these measurements were performed blind and compared tissues from experimental and control larvae grown in the same vials – see Materials and Methods), confirming that the centrosome defects were likely promoting some level of over-proliferation, presumably due to the previously described defects in asymmetric NB divisions (Basto et al., 2008; Basto et al., 2006). In support of this possibility, we could detect no significant difference in the size of

the wing discs, which grow through mostly symmetric cell divisions, in any of these lines compared to wild type (Fig. 1E).

**Strategy for comparing the global transcriptome of cells that lack or have amplified centrosomes**

We decided to analyse the global transcriptome from larval brain and imaginal disc tissues for three reasons: (1) It is easy to isolate these tissues in a highly reproducible manner from tightly staged wandering 3<sup>rd</sup> instar larvae; (2) Brains and imaginal discs are morphologically complex tissues that are polarised and are mitotically active, so might be expected to be particularly sensitive to centrosome defects; (3) As described above, *DSas-4* mutant and *SakOE* brains are capable of forming tumours in abdominal transplantation assays (Basto et al., 2008; Castellanos et al., 2008) demonstrating that centrosome defects can, at least eventually, lead to perturbations in the normal physiology of these cells.

In an attempt to minimise variations that might simply be due to inherent differences between different inbred *Drosophila* strains, we backcrossed the *DSas-4* and *DSas-6* mutant lines and the *SakOE* line to a *w<sup>67</sup>* line (a wild type line carrying a point mutation in the *white* gene) that we used here as a wild type (WT) control. Our *w<sup>67</sup>* control stock was isogenised as well, so that all flies in this stock contained nearly identical sets of chromosomes. As additional controls, we also backcrossed a different WT strain (*Oregon-R* – [*Or-R*]) and a WT strain containing a *TM6* balancer chromosome to *w<sup>67</sup>*. All backcrossing was performed for at least 5 generations, and in each generation we selected for the *Pw+* marker associated with the mutation or the transgene (or the endogenous *w+* allele in the case of the WT *Or-R* stock, or the *Tubby* marker in the case of the *TM6* balancer) and then backcrossed these flies to the original *w<sup>67</sup>* line (supplementary material Fig. S1). This allowed us to compare tissues from different genetic backgrounds that would be largely isogenic with respect to *w<sup>67</sup>* except for the region of the genome containing the P-element insertion that causes centrosome loss (in the case of the *DSas-4* or *DSas-6* mutation) or centrosome amplification (in the case of *SakOE*) (supplementary material Fig. S2).

For each genotype to be tested, brains and imaginal discs were dissected from 3 independent batches of 10 wandering 3<sup>rd</sup> instar larvae and total RNA was prepared from each batch. We performed genome-wide expression profiling using *Drosophila* Genome 2.0 GeneChips (Affymetrix, Santa Clara, California, USA) and obtained lists of differentially expressed genes between WT and test strains that displayed at least 1.5-fold differential expression and adjusted P-values corrected for multiple hypothesis testing of  $\leq 0.05$ . Array data-sets are deposited at Gene Expression Omnibus (accession no. GSE35240). We first compared *w<sup>67</sup>* to our *Or-R* WT control. The *w<sup>67</sup>* mutation was originally isolated by Lefevre in a WT *Canton-S* background (Lefevre and Wilkins, 1966) which was collected in Canton, Ohio by Calvin Bridges in the 1920s. These two strains have therefore been kept apart in various laboratories around the world for many decades. Encouragingly, we found no significant differences in the expression levels of any genes between these strains, suggesting that our isogenisation protocol had been largely effective in eliminating any variation due to inherent strain differences.

**The global transcriptome appears unaltered in *DSas-6* mutant tissues**

When we compared the transcriptome of *w<sup>67</sup>* to that of the *DSas-6* mutant strain only two genes had statistically significant

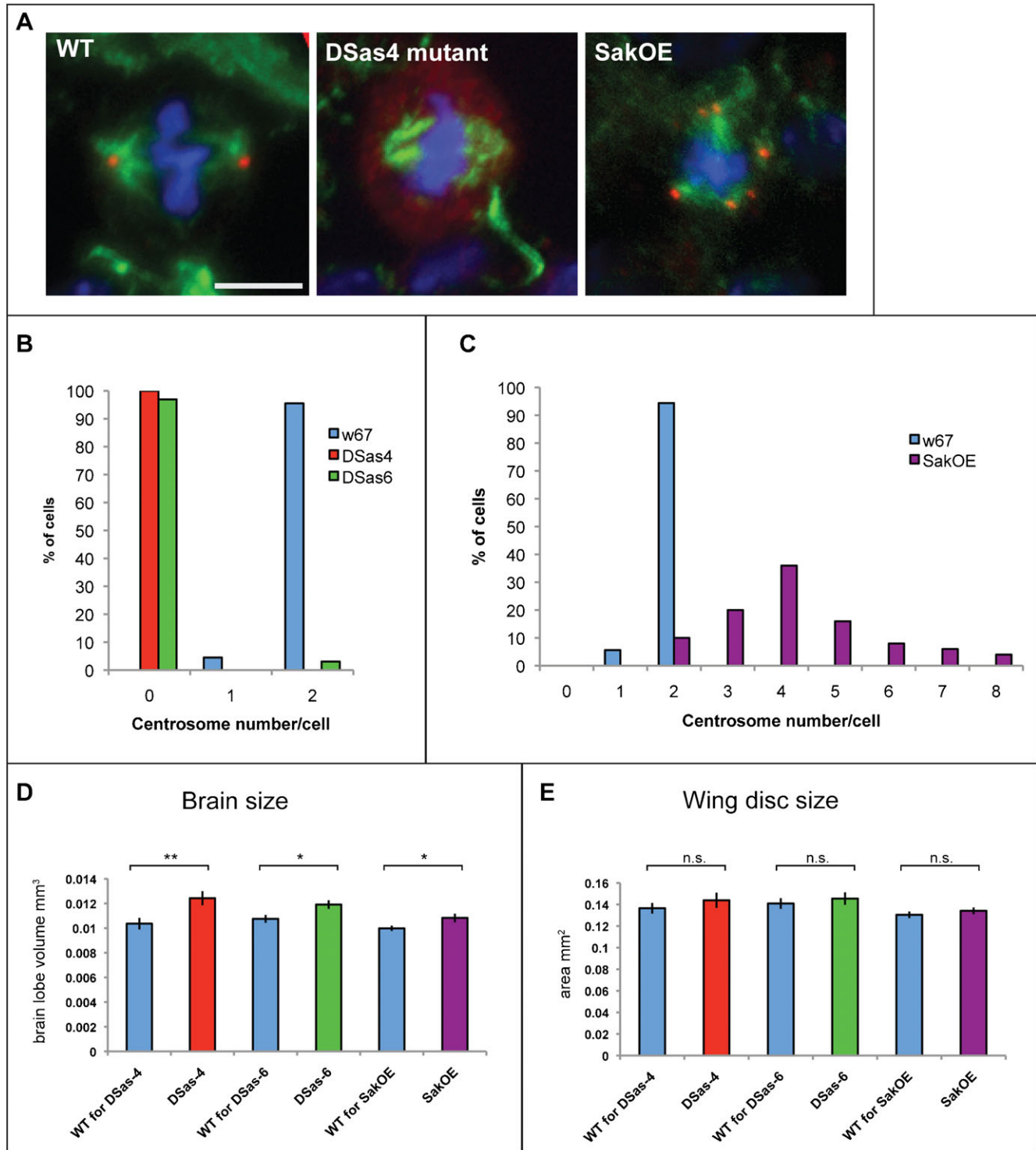


**Fig. 1. Larval brains with extra centrosomes or without centrosomes are increased in size.** (A) 3<sup>rd</sup> instar larval brain cells stained with antibodies against Asterless marking centrosomes (red) and tubulin (green). DNA is in blue. Wild type cells have two centrosomes at the spindle poles in metaphase, whereas *D-Sas4* cells do not have centrosomes. *SakOE* cells have amplified centrosomes, which can lead to multipolar spindle formation in prometaphase. Scale bar is 5  $\mu$ m. (B) Larval brains were stained with antibodies against Asterless and Centrosomin, and centrosomes were quantified in cells ( $n=295$  cells in 12 brains for *DSas-6*;  $n=381$  cells in 10 brains for *DSas-4*;  $n=246$  cells in 12 brains for *w67*). (C) Centrosomes were quantified in *SakOE* brains as described in (B) ( $n=50$  cells in 4 brains;  $n=89$  cells in 6 brains for *w67*). (D) Brain lobe circumference was measured and brain lobe volume under the assumption of the lobes being spherical was calculated in *DSas-4*, *DSas6* and *SakOE* third instar larval brains. As WT controls, *w67* larvae from the same food vial were measured for each strain (see Materials and Methods). A minimum of  $n=26$  brains were measured per strain. (E) Wing disc size was analysed by calculating the product of width  $\times$  height. Mutant wing discs were compared to WT wing discs of larvae grown in the same food vial. A minimum of  $n=22$  wing discs were measured. A t-test was performed to test for significance of the differences between mutant tissues and corresponding WT control (two asterisks stands for a P-value of  $<0.01$ ; one asterisk corresponds to a P-value of  $<0.05$ ).

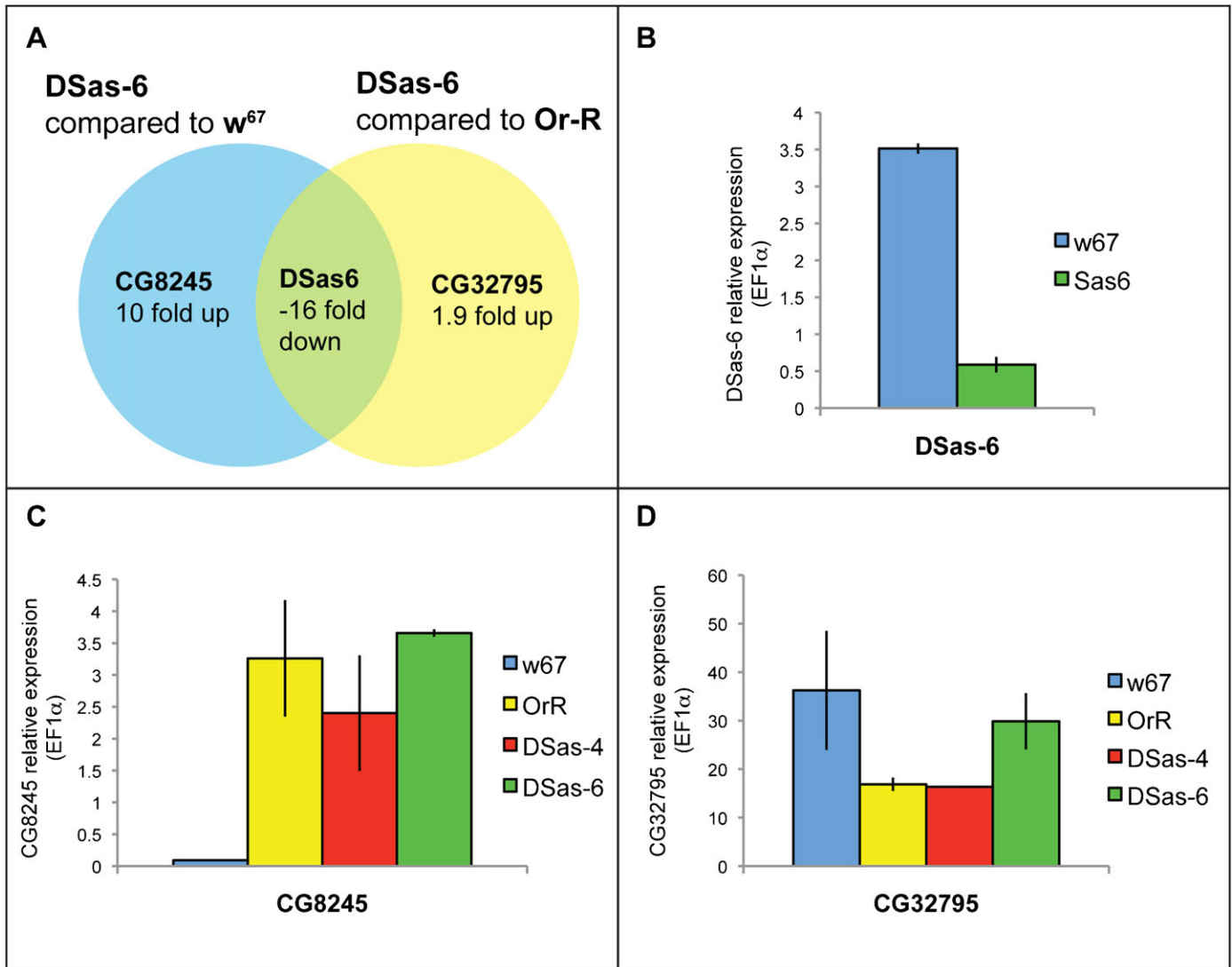


**Fig. 2. Gene expression in *DSas-6* cells.** (A) Venn diagram of significant genes in *DSas-6* cells (third instar larval brains and wing discs) compared to  $w^{67}$  and *OregonR* WT controls found in microarray analysis ( $\geq 1.5$ -fold, FDR-adj.P-value  $\leq 0.05$ ). (B–D) Confirmation of up- or down-regulation of these genes by quantitative PCR was performed using mRNA isolated from third instar larval brains and wing discs ( $n \geq 2$  independent samples). (B) mRNA levels of *DSas-6* in  $w^{67}$  and *DSas-6* mutant cells. (C) mRNA levels of *CG8245* in  $w^{67}$ , *OregonR*, *DSas-4* and *DSas-6* cells. (D) mRNA levels of *CG32795* in  $w^{67}$ , *OregonR*, *DSas-4* and *DSas-6* cells.

differences in their expression levels: *DSas-6*, which was down-regulated by  $\sim 16\times$  (FDR-adjusted P-value 0.005) and *CG8245*, which was up-regulated by  $\sim 10\times$  (FDR-adjusted P-value = 0.004). *DSas-6* was also one of only two genes identified when the *DSas-6* mutant strain was compared to the WT *Or-R* strain: it was down-regulated by  $\sim 16\times$  (FDR-adjusted P-value = 0.001), while *CG32795* was up-regulated by  $\sim 2\times$  (FDR-adjusted P-value = 0.05) (Fig. 2A). We performed quantitative RT-PCR (qRT-PCR) to test the reliability of these results. This analysis confirmed that *DSas-6* was down-regulated compared to both WT strains ( $\sim 6$  fold) (Fig. 2B). Interestingly, and in agreement with the chip data, *CG8245* was significantly up-regulated ( $\sim 40\times$ ) in *DSas-6* mutants compared to  $w^{67}$  (Fig. 2C), but not compared to *Or-R*, while *CG32794* was slightly up-regulated ( $\sim 1.8\times$ ) in *DSas-6* mutants compared to *Or-R*, but not compared to  $w^{67}$  (Fig. 2D). These results demonstrate that *CG8245* and *CG32795* are expressed at different levels in these strains, but

this difference is unlikely to be caused by the lack of centrosomes in the *DSas-6* mutant tissue as a similar difference is seen when the two WT strains are compared to each other. The different expression levels of *CG8245* and *CG32795* were also detected in the microarray comparison between  $w^{67}$  and *OrR*, although they were not scored as significant (data not shown).

These qRT-PCR experiments indicate that our chip analysis likely provides a robust and reliable comparison of the transcriptomes from these different strains. Remarkably, therefore, we conclude that there are few, if any, significant changes to the transcriptome of these *DSas-6* mutant tissues when compared to WT.

A small number of genomic regions are aberrantly expressed in *DSas-4* mutant tissues

We next compared the transcriptome of the *DSas-4* mutant strain to  $w^{67}$ . We identified 19 genes that were up-regulated and 8 genes

**Table 1. Genes significantly up- or down-regulated in DSas4 mutant cells compared to both WT controls ( $\geq 1.5$ -fold, adj.P-value  $\leq 0.05$ ).**

Gene	Map	Fold Change <sup>a</sup>	Function <sup>b</sup>
Hsc70-2	87D10-87D10	141.10	protein folding, response to heat
CG31157	87D10-87D10	23.52	unknown
CG31287	89B7-89B7	16.92	protein folding
CG9279	76B6-76B6	8.81	microtubule-based movement
miple	61B3-61B3	4.56	unknown
Ugt86Di	86D5-86D5	3.45	metabolic process
GstD3	87B8-87B8	2.25	unknown
lig3	87B9-87B9	2.08	DNA ligation, DNA replication, DNA recombination
Rbp4	86C6-86C6	1.88	mRNA processing
CG3634	77E8-77E8	1.61	unknown
TFIIFbeta	86C6-86C6	-2.07	transcription from RNA polymerase II promoter
MED7	86C5-86C5	-2.13	transcription from RNA polymerase II promoter
wnd	76B9-76B9	-2.34	protein phosphorylation
DSas-4	84C6-84C7	-6.82	centriole duplication

<sup>a</sup>Fold change compared to w67 is given<sup>b</sup>GO Term for Biological Function

that were down-regulated in the *DSas-4* mutant tissue (supplementary material Table S1). Again, we also compared *DSas-4* mutant tissue to the other WT control, *Or-R*, and identified 15 genes that were up-regulated and 7 that were down-regulated (supplementary material Table S2). We assessed the

overlap of these two lists and identified 14 genes that were differentially expressed when *DSas-4* was compared to both WT controls (Table 1; Fig. 3A). Although these 14 genes are strong candidates for genes that are differentially expressed in *DSas-4* mutant cells, they did not obviously cluster into any large

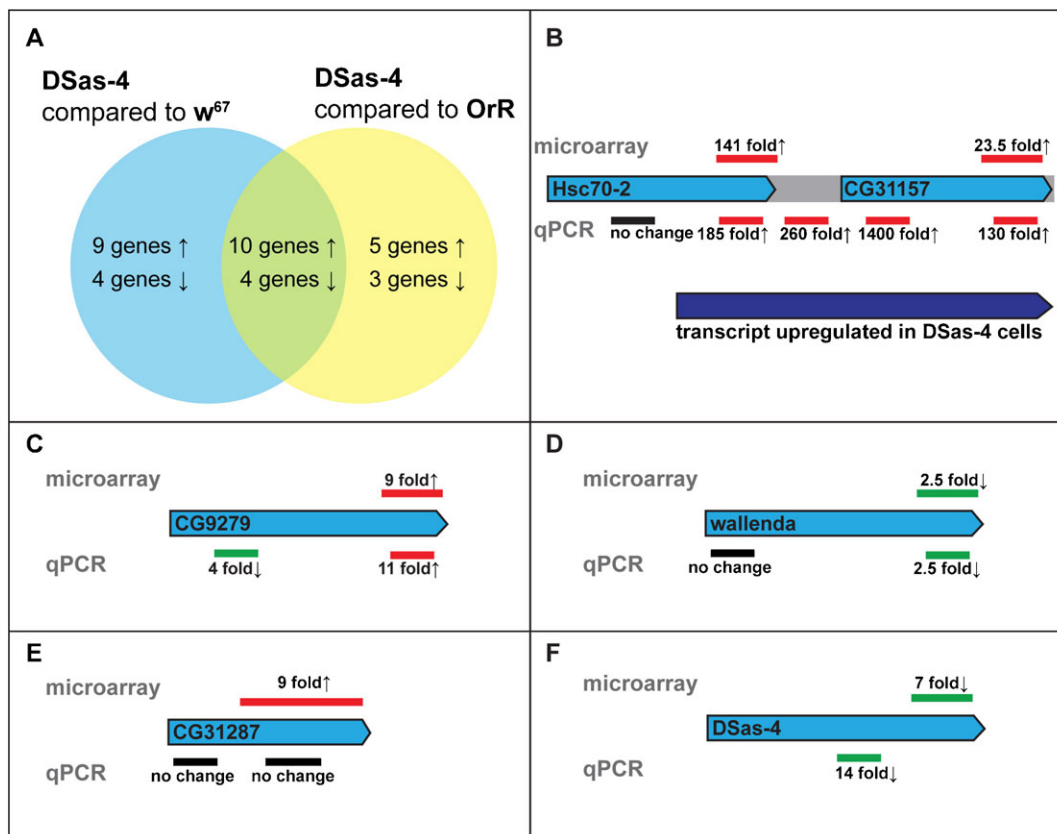


**Fig. 3. Gene expression in *DSas-4* cells.** (A) Venn diagram of significant genes in *DSas-4* cells (third instar larval brains and wing discs) compared to *w67* and *OregonR* WT controls found in microarray analysis ( $\geq 1.5$ -fold, FDR-adj.P-value  $\leq 0.05$ ). (B–F) Validation of up- and down-regulation by quantitative PCR. Fold change found in microarray analysis is shown above, and fold change found by qPCR analysis is given below the blue bar indicating the transcript. Red (up-regulation), green (down-regulation) and black (no change) bars indicate the position where microarray probes and qPCR primers bind to the transcript. (B) An unannotated transcript (dark blue), spanning the 5' end of *Hsc70-2*, the gene *CG31157* and the genomic region between the two genes, appears to be up-regulated in *DSas-4* cells.

functionally related group (Table 1). Moreover, it seems unlikely that these differences are directly caused by the lack of centrosomes in the *DSas-4* mutant cells, as none of these genes were identified as being differentially regulated in *DSas-6* mutant cells that also lack centrosomes. In addition, we noticed that several of the genes that are most differentially regulated in *DSas-4* mutant cells were located very close to one other in the genome. For example, the two most up-regulated genes, *Hsc70-2* and *CG31157*, are located directly adjacent to each other, while two of the most statistically significantly down-regulated genes (after *DSas-4* itself and *wallenda*), *Transcription factor TFIIFbeta* and *Mediator complex subunit 7 (MED7)*, are separated by only one gene, perhaps indicating that chromatin architecture may be altered in these regions in the *DSas-4* mutant cells.

To confirm whether these genes were differentially expressed in *DSas-4* mutant tissues we performed qRT-PCR experiments with the top 4 up-regulated genes (*Hsc70-2*, *CG31157*, *CG31287* and *CG9279*) and the two most down-regulated genes (*DSas-4* itself and *wallenda*). We designed qRT-PCR primers that would amplify across the region of each gene that was probed in our microarray experiments, as well as primers that would detect expression from a different region of each gene. As noted above, the two most up-regulated genes lie right next to each other in the genome and are transcribed in the same direction. To our surprise, we found that the 5' end of *HSC70-2* was not overexpressed, but the 3' end (the region probed in our chip analysis) was strongly overexpressed by ~185×, while both the 5' and 3' ends of *CG31157* were overexpressed by ~1400× and ~130×, respectively in *DSas-4* mutant tissue (Fig. 3B). We also analysed the expression levels of the small intergenic region between these genes and found that this was also overexpressed by ~260× in *DSas-4* mutant tissue. We conclude that an unusual transcript that starts in the second half of *Hsc70-2* and reads through the *CG31157* gene is highly overexpressed in *DSas-4* mutants (Fig. 3B). We observed a similar phenomenon for *CG9279* (Fig. 3C) and *wallenda* (Fig. 3D), as our qRT-PCR analysis revealed that the expression of the regions of the genes probed in our chip analysis were indeed mis-regulated, but the expression levels of a different region of each transcription unit were not. In contrast, the transcript levels of *CG31287* (Fig. 3E) were not detectably altered in qRT-PCR experiments, suggesting that this is a false positive in our chip analysis. Down-regulation of *DSas-4* mRNA in the *DSas4* mutant was also confirmed by qRT-PCR (Fig. 3F).

Taken together, these data strongly suggest that a small number of genomic regions are genuinely mis-expressed in *DSas-4* mutant cells, but at least some of this mis-expression is due to the production of aberrant transcripts that are not normally found

in WT cells. The significance of this is unclear (see Discussion), but, as these regions are not mis-expressed in *DSas-6* mutant cells, it seems unlikely that these changes are a direct result of the lack of centrosomes in *DSas-4* mutants.

#### No genes appear to be consistently mis-expressed in *DSas-6* and *DSas-4* mutant tissues

We reasoned that our failure to identify any genes that are consistently mis-expressed in tissues lacking centrosomes might be due to a high rate of false negatives, perhaps because we were setting our statistical cut-off for significance at too high a level. To test if this was the case, we compared the overlap between the 100 most significantly differentially regulated genes in *DSas-4* and *DSas-6* mutant tissue, even though most of these genes had an adjusted P-value of more than 0.05. Only 4 genes were differentially regulated in both mutants, strongly suggesting that most of these genes are unlikely to be consistently mis-expressed in cells that lack centrosomes (Table 2). Of the 4 genes that did overlap, two seemed poor candidates for genes that might be differentially regulated in cells lacking centrosomes: *CG13822* is up-regulated in *DSas-4* mutants but down-regulated in *DSas-6* mutants, while *CG32541* is only down-regulated by -1.22 and -1.4 fold in *DSas-4* and *DSas-6* mutants, respectively. *CG11357* and *pathetic* were both up-regulated in *DSas-6* and *DSas-4* mutant tissues (Table 2), but a qRT-PCR analysis again suggested that only the expression of the 3' region of each gene (the region probed in our chip analysis) was affected, while the 5' region was not. This analysis strongly supports our conclusion that a lack of centrosomes in these cells leads to the significant mis-expression of very few, if any, genes.

#### A small number of genes are differentially expressed in *SakOE* cells

To assess the effect of having too many centrosomes in cells we compared the transcriptome of *SakOE* cells to cells from the WT *w<sup>67</sup>* and *Or-R* strains. We found 55 and 57 genes, respectively, to be up- or down-regulated in the *SakOE* tissues (supplementary material Table S3, S4), and 32 of these genes were present in both comparisons (Table 3; Fig. 4A). No large functionally related group of genes appeared to be particularly enriched in this geneset (supplementary material Table S5, S6).

To test whether some of these genes were really differentially expressed in *SakOE* cells we again performed qRT-PCR experiments with several of the most up- (*CG32055*, *B52*, *CG14687*, *CG9279* and *Gram-negative bacteria binding protein 2 (GNBP2)*) or down-regulated (*Brf*, *CG11999* and *CG7900*) genes. Five of these eight genes were confirmed by the qRT-PCR analysis, which revealed that both their 5' and 3' regions were mis-expressed in the *SakOE* cells compared to the WT strains

**Table 2. Genes that are differentially regulated in both *DSas-4* and *DSas-6* among the 100 most significant genes in each genotype.**

Gene	CG11357	Pathetic	CG32541	CG13822
Fold Change <i>DSas-4</i>	8.71 ↑ (0.02 <sup>a</sup> )	6.99 ↑ (0.024 <sup>a</sup> )	-1.26 (0.055 <sup>a</sup> )	9.58 (0.065 <sup>a</sup> )
Fold Change <i>DSas-6</i>	5.31 ↑ (0.45 <sup>a</sup> )	5.31 ↑ (0.55 <sup>a</sup> )	-1.40 (1 <sup>a</sup> )	-1.18 (0.51 <sup>a</sup> )
<i>DSas-4</i> 3' qPCR	8.5 fold ↑	no change	n.d.	n.d.
<i>DSas-4</i> 5' qPCR	no change	no change	n.d.	n.d.
<i>DSas-6</i> 3' qPCR	4 fold ↑	2.6 fold ↑	n.d.	n.d.
<i>DSas-6</i> 5' qPCR	no change	no change	n.d.	n.d.

<sup>a</sup>(adjusted P-value)

**Table 3. Differentially regulated genes in SakOE cells compared to both WT controls ( $\geq 1.5$ -fold, adj.P-value  $\leq 0.05$ ).**

Gene	Map	Fold Change <sup>a</sup>	Function <sup>b</sup>
w	3B6-3B6	74.81	eye pigment biosynthetic process
CG32055	67D11-67D11	43.82	unknown
B52	87F7-87F7	14.38	nuclear mRNA splicing via spliceosome, mRNA splice site selection
CG14687	86C6-86C6	8	unknown
CG9279	76B6-76B6	7.57	microtubule-based movement
CG13032	73B6-73B6	7.3	unknown
CG5618	77B5-77B5	4.48	carboxylic acid metabolic process, proteolysis
CG31495	87F15-87F15	3.63	unknown
miple	61B3-61B3	3.47	unknown
CG7433	76D8-76E1	3.09	cellular amino acid metabolic process, gamma-aminobutyric acid metabolic process
Past1	87C6-87C6	3.07	endocytosis, germline development, imaginal disc-derived wing margin development
GNDP2	75D6-75D6	3.02	carbohydrate metabolic process, defense response
CG32939	85E4-85E4	2.32	unknown
Rbp1	86C6-86C6	2.3	nuclear mRNA splicing via spliceosome, mRNA splice site selection
CG2004	8A2-8A2	2.27	unknown
P58IPK	85D27-85D27	2.24	protein folding
SrpRbeta	66D11-66D11	2.17	neurogenesis, larval chitin based cuticle development
CG18542	85E4-85E4	1.99	unknown
p24-1	10F1-10F1	1.86	neurogenesis, post-Golgi vesicle-mediated transport
CaBP1	35F12-35F12	1.75	cell redox homeostasis, glycerol ether metabolic process
CG6951	77A3-77A4	1.71	unknown
Manf	89B13-89B13	1.67	neuron homeostasis, neuron projection development
KDELR	31E1-31E1	1.6	protein retention ER lumen
MED 7	86C5-86C5	-2.07	transcription from RNA polymerase II promoter
CG5830	72C1-72C2	-2.12	unknown
TFIIFbeta	86C6-86C6	-2.15	transcription from RNA polymerase II promoter
scaf6	73E5-73E5	-2.23	nuclear mRNA splicing via spliceosome
CG32158	73A3-73A3	-2.74	unknown
CG32027	75E2-75E2	-4.91	unknown
Brf	90A3-90A5	-7.59	Regulation of transcription from RNA polymerase III promoter
CG11999	82F10-82F10	-15.43	unknown
CG7900	84E11-84E12	-44.92	unknown

<sup>a</sup>Fold change compared to w67 is given<sup>b</sup>GO Term for Biological Function

(Fig. 4B–F). The 3'-region of *CG9279* was up-regulated (in agreement with the microarray data) but the 5' region was not (Fig. 4G) (and if anything appeared to be down-regulated) suggesting that an aberrant transcript may be produced from this genomic region in the *SakOE* cells, as we observed in several genomic regions in the *DSas-4* mutant cells. The genes *CG14687* and *B52* appeared to be false positives in our microarray analysis as either no, or only a very small, change in expression levels was detected by qRT-PCR (Fig. 4H,I). These results indicate that at least some of these 32 genes are genuinely mis-expressed in *SakOE* cells, although, as these genes do not cluster into any obvious functional pathway, it is unclear whether this mis-expression is a direct consequence of the centrosome amplification in these cells (see Discussion). Nevertheless, it is clear from this analysis that centrosome amplification does not lead to a large-scale perturbation of the transcriptome and that only a relatively small number of genes, if any, are consistently mis-regulated in cells as a result of centrosome amplification.

## Discussion

We show here that centrosome loss or amplification does not dramatically alter the global transcriptome of *Drosophila* brain or imaginal disc cells. While we have identified a small number of transcripts (~10–15) whose expression appears to be genuinely mis-regulated in *DSas-4* mutant cells, several of these appear to

be aberrant transcripts that do not encode normal proteins, and few of these genes appear to be linked by any known common function. We currently do not understand why these transcripts are mis-expressed in *DSas-4* cells, but it seems unlikely that these transcripts are components of specific pathways that are activated or inactivated in response to the lack of centrosomes, as none of these transcripts are mis-expressed in *DSas-6* mutant cells, which also lack centrosomes. Similarly, we identified a slightly larger subset of genes (~30) that appear to be mis-expressed in cells that overexpress *Sak* and so have too many centrosomes. Again, however, few of these genes appear to be linked by any known common function. Unfortunately, we have no independent way of efficiently driving centrosome amplification in brain and imaginal disc cells (independent of *Sak* overexpression), to test whether centrosome amplification is directly responsible for this transcriptional mis-regulation or whether it is due to some other change in the *SakOE* cells, as appears to be the case in *DSas-4* cells. The human homologue of *Sak*, Plk4, has been reported to phosphorylate Hand1, a transcription factor that controls cell fate (Martindill et al., 2007), perhaps explaining why more genes are differently expressed in *SakOE* cells than in cells that lack centrosomes.

While we cannot rule out that centrosome defects lead to significant post-transcriptional changes without affecting the transcription of many genes, our findings strongly suggest that

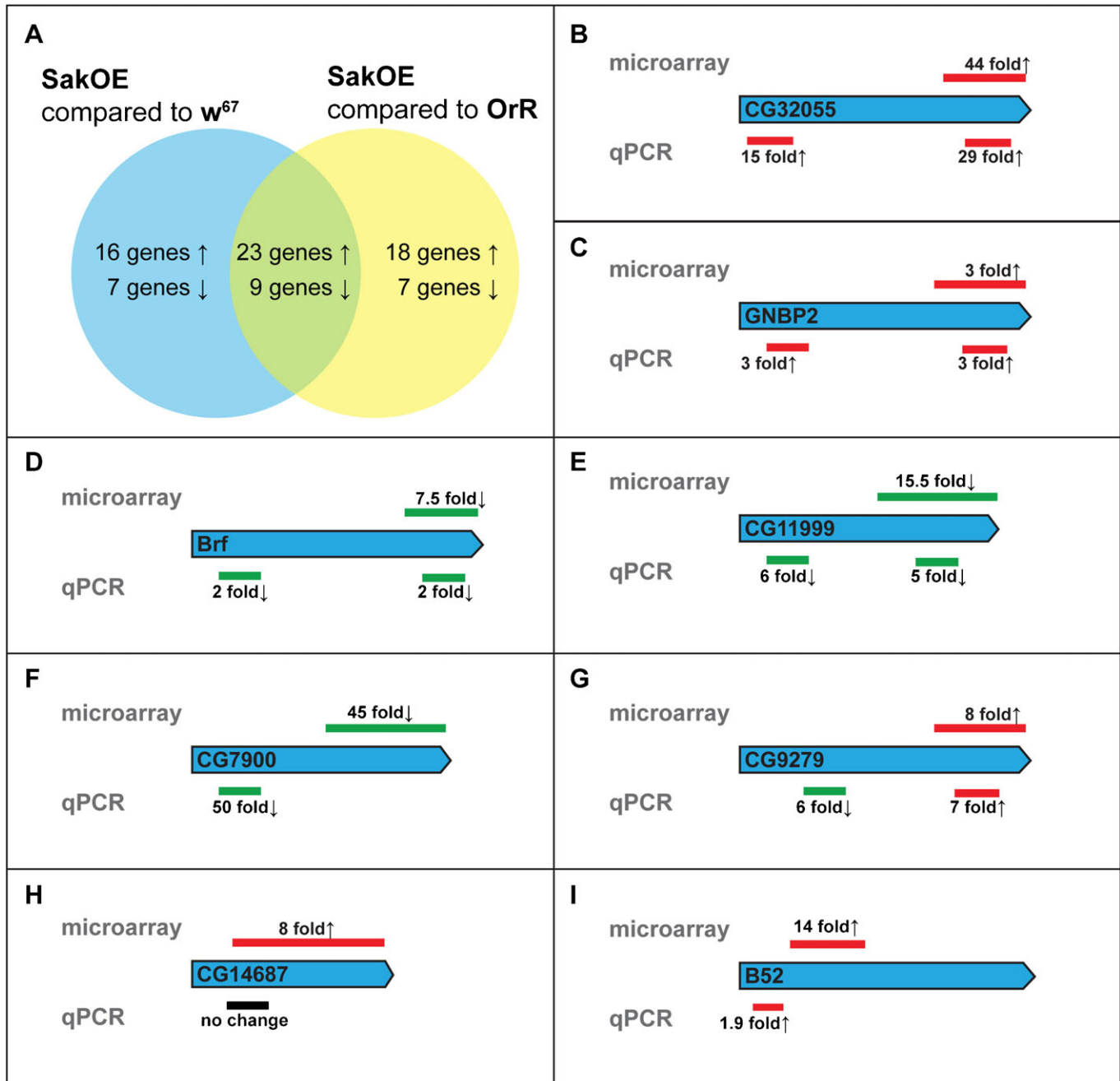


**Fig. 4. Gene expression in *SakOE* cells.** (A) Venn diagram of significant genes in *SakOE* cells (third instar larval brains and wing discs) compared to *w<sup>67</sup>* and *OregonR* WT controls found in microarray analysis ( $\geq 1.5$ -fold, adj.P-value  $\leq 0.05$ ). (B–I) Validation of up- and down-regulation by quantitative PCR. Fold change found in microarray analysis is shown above, and fold change found by qPCR analysis is given below the blue bar indicating the transcript. Red (up-regulation), green (down-regulation) and black (no change) bars indicate the position where microarray probes and qPCR primers bind to the transcript.

centrosome defects do not induce a major stress response in these cells. This finding is important, as centrosome defects appear to be a source of stress to cells *in vitro* (Mikule et al., 2007; Srsen et al., 2006; Uetake et al., 2007), where they have been shown to activate a stress response via the p38 and p53 pathways. It is not known what effect the activation of these pathways might have on gene expression in *Drosophila*, but genome wide expression studies in mammalian cells have shown that p38 stress-activated protein kinase activation leads to changes in expression of many genes, some of which are transcription factors (Ferreiro et al.,

2010). Our GO enrichment analysis does not show enrichment of any known stress response genes in response to centrosome defects. Thus, although cellular stress has been linked to tumorigenesis in some *Drosophila* models (Rossi and Gonzalez, 2011; Wu et al., 2010), it appears unlikely to be an important driver of tumorigenesis in flies with centrosome defects.

If centrosome defects *per se* do not result in dramatic changes in cell physiology, then why are *Drosophila* brain cells without centrosomes or with amplified centrosomes predisposed to form

tumours (Basto et al., 2008; Castellanos et al., 2008)? It is known that spindle assembly is slow in cells that have lost their centrosomes or have extra centrosomes, and this leads to a relatively modest increase in chromosome segregation errors (Basto et al., 2008; Basto et al., 2006; Ganem et al., 2009). Aneuploidy has long been thought to contribute to tumorigenesis (Boveri, 2008) and although mutations that lead to large-scale chromosomal instability do not seem to drive tumour formation in flies (Castellanos et al., 2008), it is possible that the low-level of aneuploidy induced by centrosome defects is actually a more effective driver of cancer (Weaver et al., 2007). Alternatively, although most fly cells with centrosome defects appear to divide relatively normally, it has previously been shown that such asymmetrically dividing brain NB divide symmetrically ~10–15% of the time, as the astral MTs generated by centrosomes in these cells help the spindle to efficiently align with cortical cell fate determinants (Basto et al., 2008; Basto et al., 2006). This appears to lead to an expansion of the NB pool, consistent with the increase in brain size that we report here.

Our transcriptional profiling experiments, however, show that this brain overgrowth is likely to be benign as it leads to few, if any, changes in gene expression. The NBs that accumulate in these brains are therefore unlikely to be malignant – whereas the tumours formed from these brains in abdominal transplantations clearly are malignant, as they show immortality, aneuploidy and the ability to metastasise (Basto et al., 2008; Castellanos et al., 2008; Caussinus and Gonzalez, 2005), all of which almost certainly require large-scale changes in gene expression (Ramaswamy et al., 2003; Rhodes et al., 2004; Scott et al., 2011). We conclude that in brain tissues with centrosome defects, an additional step must lie between the generation of overgrowing, but physiologically normal brains, and the tumours that can eventually be formed from these brains in transplantation experiments. An attractive possibility is that the overproliferation of NBs leads to a bigger stem cell pool and larger brains, but that the low level of chromosomal missegregation facilitates the generation of mutations that occasionally lead to the generation of a malignant stem cell, which ultimately drives tumour formation.

This model has obvious similarities to the cancer stem cell (CSC) theory. A correlation between CSC and chromosomal instability has been suggested (Lagasse, 2008; Li et al., 2009) and recent studies have indicated that aneuploidy and CSCs models of cancer are not mutually exclusive (Conway et al., 2009; Liang et al., 2010). It will be interesting to test whether low level aneuploidy in cells without centrosomes or with too many centrosomes leads to the accumulation of mutations in NBs *in vivo*. Transcriptional profiling experiments on single cells could answer this question in the future.

## Materials and Methods

### Fly strains

The following mutant alleles were used in this study: *DSas-4<sup>2214</sup>* (Basto et al., 2006) *DSas-6<sup>02901</sup>* (Rodrigues-Martins et al., 2007). Overexpression of *Sak* in the *SakOE* strain is caused by the ubiquitin-promoter driven expression of *GFP-Sak* (Basto et al., 2008). Laboratory *w<sup>67</sup>* and *Oregon-R* strains were used as wild type controls.

### Immunofluorescent staining and quantification of centrosome numbers in larval brains

For immunofluorescent staining, brains of third instar larvae were dissected in PBS and fixed in PBS + 4% Formaldehyde in PBS for 20 minutes. Brains were transferred to 45% acetic acid for 15 seconds and then to 60% acetic acid on a

coverslip for 3 min. Then the brains were squashed between a slide and the coverslip and flash frozen in liquid nitrogen. Coverslips were removed, and the slides were placed in 100% methanol for 5 minutes. Samples were rehydrated in PBT for 1 h and then incubated with primary antibodies under a mounted coverslip in a moist chamber overnight at 4°C. On the next day the slides were washed in PBT and incubated with the secondary antibodies for three hours. After incubation the slides were washed in PBT, stained for 10 minutes in Hoechst33258 (Life Technologies, Carlsbad, California, USA) and then mounted in mounting medium (85% glycerol and 2.5% n-propylgallate). Slides were observed on a Zeiss Axioskop 2 microscope (Carl Zeiss, Ltd., Welwyn Garden City, Hertfordshire, UK) with a CoolSNAP HQ camera (Photometrics, Tucson, Arizona, USA), using a 63×/1.25 NA objective (Carl Zeiss, Ltd., Welwyn Garden City, Hertfordshire, UK) with Immersol oil (Carl Zeiss, Ltd., Welwyn Garden City, Hertfordshire, UK). Images were acquired using Metamorph software (Molecular Devices, Sunnyvale, California, USA), imported into Photoshop CS2 (Adobe, San Jose, California, USA), and adjusted to use the full range of pixel intensities. Neuroblasts and ganglion mother cells were scored in prophase in order to ensure that centrosomes were duplicated but extra centrosomes would not be clustered at the spindle poles. These cells were identified using DNA morphology and dots were scored as centrosomes only if they co-stained for Cnn and Asl.

### Antibodies

For quantification of centrosomes in brain cells, the following primary antibodies were used at a 1:500 dilution: rabbit anti-Asl (Conduit et al., 2010) and guinea pig anti-Cnn (Lucas and Raff, 2007). Alexa488 anti-guinea pig and Alexa568 anti-rabbit secondary antibodies were used at a 1:1000 dilution (Molecular Probes, Life Technologies, Carlsbad, California, USA). For stainings of spindle and centrosomes, rabbit anti-Asl and mouse monoclonal anti- $\alpha$ -tubulin (DM1a, Sigma-Aldrich, St. Louis, Missouri, USA) were used as primary antibodies (1:500), and Alexa568 anti-rabbit and Alexa488 anti-mouse (1:1000) as secondary antibodies (Molecular Probes, Life Technologies, Carlsbad, California, USA).

### Measurement of brain and imaginal disc size

*DSas-4*, *DSas-6* and *SakOE* strains were recombined with a *Hand*-GFP transgene that is expressed in the larval cardiac tissue (Han et al., 2006). *w<sup>67</sup>* fertilised females were put together with an equal number of either *sakOE*, *Hand*>GFP, *DSas-6,Hand*>GFP/TM6C or *DSas-4,Hand*>GFP/TM6C fertilised females and these females were allowed to lay eggs for a maximum of 12 hours. A few days later, brains and wing discs of wandering third instar larvae were dissected and pictures were taken with a Nikon DS-F1 camera mounted on a Nikon SMZ800 dissecting microscope (Nikon, Kingston Upon Thames, Surrey, UK); the circumference of the brain lobes and the width and height of the wing discs were then measured in ImageJ (Abramoff et al., 2004). After making these measurements, the genotype of the tissue that had been measured was checked by examining the larval carcass for *Hand*-GFP expression. In this way we ensured that the analysis was performed blind, and that the mutant (or *Sak*-overexpressing) and WT larvae were grown under identical conditions in the same vial. Brain and wing disc sizes of at least 20 animals were measured per data-point and the average and standard error were calculated. A Student's t-test was performed to calculate P-values.

### Microarray analysis

Transcriptional profiles of wild type flies, *DSas-4* flies, *DSas-6* flies and *SakOE* flies were generated. Total RNA of brains and imaginal discs from 10 third instar larvae per sample was isolated using TRIzol (Life Technologies, Carlsbad, California, USA) chloroform extraction and isopropanol precipitation. For each strain three independent samples were analysed. Purity and integrity of the purified RNA was assessed on the Agilent Bioanalyzer 2100 (Agilent, Santa Clara, California, USA). Concentration was determined with a Nanodrop ND-1000 Spectrophotometer (Nanodrop Technologies, Wilmington, Delaware, USA). 500 ng RNA per sample was processed to labelled cRNA using the Affymetrix 3' IVT Express kit according to the manufacturer's instructions and hybridised to Affymetrix *Drosophila* 2.0 GeneChips for 16 hrs at 45°C. Gene chips were washed and stained with streptavidin-phycoerythrin using the Affymetrix Fluidics Station 450 and scanned on an Affymetrix GeneChip 3000 scanner (all Affymetrix, Santa Clara, California, USA). Quality control of microarray expression data was performed using the Bioconductor package AffyPLM (Gautier et al., 2004). Probe intensities from Affymetrix image files ("CEL" files) were normalised using quantile normalisation (Bolstad et al., 2003), and expression signals of all genes (probesets) were calculated using GCRMA (Guanosine Cytidine robust multiarray analysis) (Wu and Irizarry, 2007). Differentially expressed genes between WT and Experimental samples were identified using the Bioconductor package limma (Smyth, 2005). We obtained lists of genes that displayed at least 1.5-fold change in expression and a Benjamini-Hochberg FDR-corrected P-value of  $\leq 0.05$  (Benjamini and Hochberg, 2005). We analysed the list of differentially expressed genes of *SakOE* compared to *w<sup>67</sup>* for enrichment of Gene Ontology (GO) terms using DAVID, a program that weighs the enrichment of a specific GO

term in a given data-set relative to the frequency of that term on the *Drosophila* 2.0 chip (Dennis et al., 2003; Huang et al., 2008). We were looking for enrichment in the GO FAT set, which attempts to filter the broadest terms so that they do not overshadow the more specific terms. Raw data can be accessed in Gene Expression Omnibus (<http://www.ncbi.nlm.nih.gov/geo>; accession number GSE35240).

### Quantitative PCR analysis

For qPCR analysis RNA was isolated as described for the microarray experiments. 1 µg RNA was treated with DNaseI (Invitrogen life technologies) and used for reverse transcription with the Transcriptor High Fidelity cDNA Synthesis Kit (Roche Diagnostics Ltd., Burgess Hill, West Sussex, UK) using oligo(dT) primer. cDNA was diluted 1:2 and 1 µl diluted cDNA was used for qPCR analysis using the SensiMix SYBR No-ROX Kit (Bioline Reagents Ltd, London, UK) in a MJ Research PTC-200 thermal cycler with a Chromo4 detector (both Biorad, Hercules, California, USA). Genespecific primers for qPCR analysis were designed using PerlPrimer (Marshall, 2004) (supplementary material Table S7). Expression of the tested genes was measured in triplicates and gene expression levels for each individual sample were normalised expression of *EF1a*. At least 2 independent samples were measured per gene. Mean relative gene expression was determined and expressed as  $2^{-\Delta CT}$  ( $\Delta CT = (CT_{\text{gene}} - CT_{\text{EF1alpha}}) \times 1000$ ) (Livak and Schmittgen, 2001).

### Acknowledgements

We thank members of the Raff Lab for critical reading of the manuscript and stimulating discussions. We are grateful to Christopher Dooley and Markus Grohme for comments on the manuscript and experimental advice. We would like to thank Andrew Renault for sharing the Hand-GFP fly stock. This work was supported by a EPA Trust studentship to J.B., a National Institutes of Health Fellowship [F32 GM 80924-02] to M.P.L. and Cancer Research UK Programme Grant [10530] to J.W.R.

### Competing Interests

The authors have no competing interests to declare.

### References

- Abramoff, M. D., Magalhães, P. J. and Ram, S. J. (2004). Image processing with ImageJ. *Biophotonics International* **11**, 36-42.
- Alkurayf, F. S., Cai, X., Emery, C., Mochida, G. H., Al-Dosari, M. S., Felie, J. M., Hill, R. S., Barry, B. J., Partlow, J. N., Gascon, G. G. et al. (2011). Human mutations in NDE1 cause extreme microcephaly with lissencephaly. *Am. J. Hum. Genet.* **88**, 536-547.
- Bakircioglu, M., Carvalho, O. P., Khurshid, M., Cox, J. J., Tuysuz, B., Barak, T., Yilmaz, S., Caglayan, O., Dincer, A., Nicholas, A. K. et al. (2011). The essential role of centrosomal NDE1 in human cerebral cortex neurogenesis. *Am. J. Hum. Genet.* **88**, 523-535.
- Basto, R., Lau, J., Vinogradova, T., Gardiol, A., Woods, C. G., Khodjakov, A. and Raff, J. W. (2006). Flies without centrioles. *Cell* **125**, 1375-1386.
- Basto, R., Brunk, K., Vinadogrova, T., Peel, N., Franz, A., Khodjakov, A. and Raff, J. W. (2008). Centrosome amplification can initiate tumorigenesis in flies. *Cell* **133**, 1032-1042.
- Bello, B., Reichert, H. and Hirth, F. (2006). The brain tumor gene negatively regulates neural progenitor cell proliferation in the larval central brain of *Drosophila*. *Development* **133**, 2639-2648.
- Benjamini, Y. and Hochberg, Y. (2005). Controlling the false discovery rate: a practical and powerful approach to multiple testing. *J. R. Stat. Soc. Ser. A Stat. Soc.* **57**, 289-300.
- Betschinger, J., Mechtler, K. and Knoblich, J. A. (2006). Asymmetric segregation of the tumor suppressor brat regulates self-renewal in *Drosophila* neural stem cells. *Cell* **124**, 1241-1253.
- Bolstad, B. M., Irizarry, R. A., Astrand, M. and Speed, T. P. (2003). A comparison of normalization methods for high density oligonucleotide array data based on variance and bias. *Bioinformatics* **19**, 185-193.
- Bond, J. and Woods, C. G. (2006). Cytoskeletal genes regulating brain size. *Curr. Opin. Cell Biol.* **18**, 95-101.
- Boveri, T. (2008). Concerning the origin of malignant tumours by Theodor Boveri. Translated and annotated by Henry Harris. *J. Cell Sci.* **121 Suppl 1**, 1-84.
- Carney, T. D., Miller, M. R., Robinson, K. J., Bayraktar, O. A., Osterhout, J. A. and Doe, C. Q. (2012). Functional genomics identifies neural stem cell sub-type expression profiles and genes regulating neuroblast homeostasis. *Dev. Biol.* **361**, 137-146.
- Castellanos, E., Dominguez, P. and Gonzalez, C. (2008). Centrosome dysfunction in *Drosophila* neural stem cells causes tumors that are not due to genome instability. *Curr. Biol.* **18**, 1209-1214.
- Causinus, E. and Gonzalez, C. (2005). Induction of tumor growth by altered stem-cell asymmetric division in *Drosophila melanogaster*. *Nat. Genet.* **37**, 1125-1129.
- Conduit, P. T., Brunk, K., Dobbelaere, J., Dix, C. I., Lucas, E. P. and Raff, J. W. (2010). Centrioles regulate centrosome size by controlling the rate of Cnn incorporation into the PCM. *Curr. Biol.* **20**, 2178-2186.
- Conway, A. E., Lindgren, A., Galic, Z., Pyle, A. D., Wu, H., Zack, J. A., Pelligrini, M., Teitell, M. A. and Clark, A. T. (2009). A self-renewal program controls the expansion of genetically unstable cancer stem cells in pluripotent stem cell-derived tumors. *Stem Cells* **27**, 18-28.
- Dennis, G., Jr, Sherman, B. T., Hosack, D. A., Yang, J., Gao, W., Lane, H. C. and Lempicki, R. A. (2003). DAVID: Database for Annotation, Visualization, and Integrated Discovery. *Genome Biol.* **4**, P3.
- Doe, C. Q. (2008). Neural stem cells: balancing self-renewal with differentiation. *Development* **135**, 1575-1587.
- Doxsey, S., Zimmerman, W. and Mikule, K. (2005). Centrosome control of the cell cycle. *Trends Cell Biol.* **15**, 303-311.
- Ferreiro, I., Joaquin, M., Islam, A., Gomez-Lopez, G., Barragan, M., Lombardía, L., Domínguez, O., Pisano, D. G., Lopez-Bigas, N., Nebreda, A. R. et al. (2010). Whole genome analysis of p38 SAPK-mediated gene expression upon stress. *BMC Genomics* **11**, 144.
- Ganem, N. J., Godinho, S. A. and Pellman, D. (2009). A mechanism linking extra centrosomes to chromosomal instability. *Nature* **460**, 278-282.
- Gautier, L., Cope, L., Bolstad, B. M. and Irizarry, R. A. (2004). Affy-analysis of Affymetrix GeneChip data at the probe level. *Bioinformatics* **20**, 307-315.
- Gonzalez, C. (2007). Spindle orientation, asymmetric division and tumour suppression in *Drosophila* stem cells. *Nat. Rev. Genet.* **8**, 462-472.
- Gonzalez, C. (2008). Centrosome function during stem cell division: the devil is in the details. *Curr. Opin. Cell Biol.* **20**, 694-698.
- Han, Z., Yi, P., Li, X. and Olson, E. N. (2006). Hand, an evolutionarily conserved bHLH transcription factor required for *Drosophila* cardiogenesis and hematopoiesis. *Development* **133**, 1175-1182.
- Hsu, L. C. and White, R. L. (1998). BRCA1 is associated with the centrosome during mitosis. *Proc. Natl. Acad. Sci. USA* **95**, 12983-12988.
- Huang, D.-W., Sherman, B. T. and Lempicki, R. A. (2008). Systematic and integrative analysis of large gene lists using DAVID bioinformatics resources. *Nat. Protoc.* **4**, 44-57.
- Janic, A., Mendizabal, L., Llamazares, S., Rossell, D. and Gonzalez, C. (2010). Ectopic expression of germline genes drives malignant brain tumor growth in *Drosophila*. *Science* **330**, 1824-1827.
- Knoblich, J. A. (2008). Mechanisms of asymmetric stem cell division. *Cell* **132**, 583-597.
- Knoblich, J. A. (2010). Asymmetric cell division: recent developments and their implications for tumour biology. *Nat. Rev. Mol. Cell Biol.* **11**, 849-860.
- Lagasse, E. (2008). Cancer stem cells with genetic instability: the best vehicle with the best engine for cancer. *Gene Ther.* **15**, 136-142.
- Lee, C.-Y., Andersen, R. O., Cabernard, C., Manning, L., Tran, K. D., Lanskey, M. J., Bashirullah, A. and Doe, C. Q. (2006a). *Drosophila* Aurora-A kinase inhibits neuroblast self-renewal by regulating aPKC/Numb cortical polarity and spindle orientation. *Genes Dev.* **20**, 3464-3474.
- Lee, C. Y., Wilkinson, B. D., Siegrist, S. E., Wharton, R. P. and Doe, C. Q. (2006b). Brat is a Miranda cargo protein that promotes neuronal differentiation and inhibits neuroblast self-renewal. *Dev. Cell* **10**, 441-449.
- Lefevre, G. and Jr and Wilkins, M. D. (1966). Cytogenetic studies on the white locus in *Drosophila melanogaster*. *Genetics* **53**, 175-187.
- Li, L., Borodyansky, L. and Yang, Y. (2009). Genomic instability en route to and from cancer stem cells. *Cell Cycle* **8**, 1000-1002.
- Liang, Y., Zhong, Z., Huang, Y., Deng, W., Cao, J., Tsao, G., Liu, Q., Pei, D., Kang, T. and Zeng, Y.-X. (2010). Stem-like cancer cells are inducible by increasing genomic instability in cancer cells. *J. Biol. Chem.* **285**, 4931-4940.
- Lingle, W. L., Barrett, S. L., Negron, V. C., D'Assoro, A. B., Boeneman, K., Liu, W., Whitehead, C. M., Reynolds, C. and Salisbury, J. L. (2002). Centrosome amplification drives chromosomal instability in breast tumor development. *Proc. Natl. Acad. Sci. USA* **99**, 1978-1983.
- Livak, K. J. and Schmittgen, T. D. (2001). Analysis of relative gene expression data using real-time quantitative PCR and the  $2^{-\Delta\Delta CT}$  method. *Methods* **25**, 402-408.
- Löffler, H., Bochtler, T., Fritz, B., Tews, B., Ho, A. D., Lukas, J., Bartek, J. and Krämer, A. (2007). DNA damage-induced accumulation of centrosomal Chk1 contributes to its checkpoint function. *Cell Cycle* **6**, 2541-2548.
- Lucas, E. P. and Raff, J. W. (2007). Maintaining the proper connection between the centrioles and the pericentriolar matrix requires *Drosophila* centrosomin. *J. Cell Biol.* **178**, 725-732.
- Marshall, O. J. (2004). PerlPrimer: cross-platform, graphical primer design for standard, bisulphite and real-time PCR. *Bioinformatics* **20**, 2471-2472.
- Martindill, D. M., Risebro, C. A., Smart, N., Franco-Viseras, M. M., Rosario, C. O., Swallow, C. J., Dennis, J. W. and Riley, P. R. (2007). Nucleolar release of Hand1 acts as a molecular switch to determine cell fate. *Nat. Cell Biol.* **9**, 1131-1141.
- Mikule, K., Delaval, B., Kaldis, P., Jurczyk, A., Hergert, P. and Doxsey, S. (2007). Loss of centrosome integrity induces p38-p53-p21-dependent G1-S arrest. *Nat. Cell Biol.* **9**, 160-170.
- Peel, N., Stevens, N. R., Basto, R. and Raff, J. W. (2007). Overexpressing centriole-replication proteins *in vivo* induces centriole overduplication and *de novo* formation. *Curr. Biol.* **17**, 834-843.
- Pihan, G. A., Wallace, J., Zhou, Y. and Doxsey, S. J. (2003). Centrosome abnormalities and chromosome instability occur together in pre-invasive carcinomas. *Cancer Res.* **63**, 1398-1404.

- Ramaswamy, S., Ross, K. N., Lander, E. S. and Golub, T. R. (2003). A molecular signature of metastasis in primary solid tumors. *Nat. Genet.* **33**, 49-54.
- Rhodes, D. R., Yu, J., Shanker, K., Deshpande, N., Varambally, R., Ghosh, D., Barrette, T., Pandey, A. and Chinnaiyan, A. M. (2004). Large-scale meta-analysis of cancer microarray data identifies common transcriptional profiles of neoplastic transformation and progression. *Proc. Natl. Acad. Sci. USA* **101**, 9309-9314.
- Rodrigues-Martins, A., Bettencourt-Dias, M., Riparbelli, M., Ferreira, C., Ferreira, I., Callaini, G. and Glover, D. M. (2007). DSAS-6 organizes a tube-like centriole precursor, and its absence suggests modularity in centriole assembly. *Curr. Biol.* **17**, 1465-1472.
- Rossi, F. and Gonzalez, C. (2011). Synergism between altered cortical polarity and the PI3K/TOR pathway in the suppression of tumour growth. *EMBO Rep.* **13**, 157-162.
- Scott, K. L., Nogueira, C., Heffernan, T. P., van Doorn, R., Dhakal, S., Hanna, J. A., Min, C., Jaskeliouff, M., Xiao, Y., Wu, C. J. et al. (2011). Proinvasion metastasis drivers in early-stage melanoma are oncogenes. *Cancer Cell* **20**, 92-103.
- Smyth, G. K. (2005). Limma: linear models for microarray data. In *Bioinformatics And Computational Biology Solutions Using R And Bioconductor* (ed. R. Gentleman, V. Carey, S. Dudoit, R. Irizarry and W. Huber), pp. 397-420. New York: Springer.
- Srsen, V., Gnad, N., Dammermann, A. and Merdes, A. (2006). Inhibition of centrosome protein assembly leads to p53-dependent exit from the cell cycle. *J. Cell Biol.* **174**, 625-630.
- Takada, S., Kwak, S., Koppetsch, B. S. and Theurkauf, W. E. (2007). *grp (chk1)* replication-checkpoint mutations and DNA damage trigger a Chk2-dependent block at the *Drosophila* midblastula transition. *Development* **134**, 1737-1744.
- Tritarelli, A., Oricchio, E., Ciciarello, M., Mangiacasale, R., Palena, A., Lavia, P., Soddu, S. and Cundari, E. (2004). p53 localization at centrosomes during mitosis and postmitotic checkpoint are ATM-dependent and require serine 15 phosphorylation. *Mol. Biol. Cell* **15**, 3751-3757.
- Uetake, Y., Loncarek, J., Nordberg, J. J., English, C. N., La Terra, S., Khodjakov, A. and Sluder, G. (2007). Cell cycle progression and de novo centriole assembly after centrosomal removal in untransformed human cells. *J. Cell Biol.* **176**, 173-182.
- Wang, H., Somers, G. W., Bashirullah, A., Heberlein, U., Yu, F. and Chia, W. (2006). Aurora-A acts as a tumor suppressor and regulates self-renewal of *Drosophila* neuroblasts. *Genes Dev.* **20**, 3453-3463.
- Weaver, B. A. A., Silk, A. D., Montagna, C., Verdier-Pinard, P. and Cleveland, D. W. (2007). Aneuploidy acts both oncogenically and as a tumor suppressor. *Cancer Cell* **11**, 25-36.
- Wu, M., Pastor-Pareja, J. C. and Xu, T. (2010). Interaction between Ras<sup>V12</sup> and scribbled clones induces tumour growth and invasion. *Nature* **463**, 545-548.
- Wu, Z. and Irizarry, R. A. (2007). A statistical framework for the analysis of microarray probe-level data. *Ann. Appl. Stat.* **1**, 333-357.